On the determination of the at-rest lateral earth pressure coefficient and the state parameter using pushed-in high-resolution Pressuremeters

Rafael Martinez[1#], *Maximiliano Jara*[1], *Fernando Schnaid*[2] *and Gonzalo Montalva*[3]

[1]*Pangea Geotecnia, Concepción, Chile*
[2]*Universidade Federal do Rio Grande do Sul, Civil Engineering, Porto Alegre, Brazil*
[3]*Universidad de Concepción, Civil Engineering, Concepción, Chile*
[#]*Corresponding author: Rafael.martinez@pangealtda.cl*

ABSTRACT

The state parameter and the at-rest lateral earth pressure coefficient (K_0) are fundamental and critical soil parameters for evaluating liquefaction, deformations and stresses around geotechnical structures such as dams, tunnels and retaining walls. Despite their importance, their in-situ determination remains one of the most challenging aspects of geotechnical characterisation. This study presents a methodology that integrates pushed-in, high-resolution pressuremeters, finite element modelling and artificial intelligence for determining these two parameters, in spite of the disturbance produced during installation. A cylindrical steel chamber was utilised to accurately control the soil and testing conditions. Initially, the pressuremeter was installed prior to soil placement to create an ideal installation conditions, allowing undisturbed measurement of the at rest lateral earth pressure. Subsequently, the instrument was removed and re-installed by pushing it into the same prepared soil sample. A loose soil condition was achieved through dry pluviation using a controlled clean sand. Additionally, three well documented literature case studies were also analysed, including a self-boring pressuremeter and other two cone pressuremeters (pushed-in pressuremeters). For every case, the pressuremeter curves were interpreted using the Clay and Sand Constitutive model. The interpreted K_0 and state parameter values showed good agreement with the measured values, demonstrating the method validity. Hence, the present study lays a foundation for enhancing the precision of soil characterisation and improvement for analysis and design of geotechnical structures.

RESUME

Le paramètre d'état et le coefficient de pression latérale des terres au repos (K_0) sont paramètres fondamentaux et critiques du sol pour évaluer la liquéfaction, les déformations et les contraintes autour des structures géotechniques telles que les barrages, les tunnels et les murs de soutènement. Malgré leur importance, leur détermination in situ demeure l'un des aspects les plus complexes de la caractérisation géotechnique. Cette étude présente une méthodologie qui intègre des pressiomètres à haute résolution enfoncés dans le sol, la modélisation par éléments finis et l'intelligence artificielle pour déterminer ces deux paramètres, malgré les perturbations induites lors de l'installation. Une chambre cylindrique en acier a été utilisée afin de contrôler précisément les conditions du sol et des essais. Dans un premier temps, le pressiomètre a été installé avant la mise en place du sol afin de créer des conditions d'installation idéales, permettant une mesure non perturbée de la pression latérale au repos. Par la suite, l'instrument a été retiré puis réinstallé en l'enfonçant dans le même échantillon de sol préparé. Une condition de sol lâche a été obtenue par pluviation à sec à l'aide d'un sable propre et contrôlé. En complément, trois études de cas bien documentées dans la littérature ont également été analysées, incluant un pressiomètre auto-foreur et deux autres pressiomètres à cône (pressiomètres enfoncés). Pour chaque cas, les courbes pressiométriques ont été interprétées à l'aide du modèle constitutif Clay and Sand. Les valeurs de K_0 et du paramètre d'état interprétées ont montré une bonne concordance avec les valeurs mesurées, démontrant ainsi la validité de la méthode. Ainsi, la présente étude jette les bases d'une amélioration de la précision de la caractérisation des sols et du perfectionnement de l'analyse et de la conception des structures géotechniques.

Keywords: state parameter; K_0; artificial intelligence; finite elements; pressuremeter

1. Introduction

Pressuremeter tests have been used since the 1930's but gained popularity with the Ménard pressuremeter in the 1950's (Mair & Wood, 1987). The general principle of the Ménard pressuremeter test is to insert a cylindrical probe equipped with an expandable flexible membrane into a borehole into the ground. The probe is expanded following a predefined loading program, and the ground responds to the applied load yielding a cavity pressure versus cavity volumetric strain curve. This curve is called a cavity expansion curve and it can be interpreted to derive deformability and strength parameters of the ground. The resulting parameters can be used in many ways, such as to estimate foundation design parameters. The test interpretation relies either on a theoretical

analytical background, or on semi-empirical correlations. In practice, the Ménard pressuremeter interpretation is mostly empirical for the reason it will be explained below. In the 1970's Cambridge University researched into a new type of pressuremeters equipped with strain gauges rather than volume gauges which permitted the development of the self-boring pressuremeter and the push-in pressuremeter, these devices allow for the measurement of strains with a resolution of 1 micron ($1x10^{-3}$mm), i.e., about 100 times smaller than the thickness of a sheet of paper. Although this difference from the Ménard device may appear to be minor, it has a significant impact on the interpretation of the results based on fundamental concepts of soil mechanics. As the soil structure is non homogeneous and the pressuremeter cavity load produces small irregularities along its length (Houlsby & Carter, 1993; Ajalloeian & Yu, 1998) the horizontal displacements measured along the cavity are not all equal, hence, when using a Ménard device only an average horizontal strain along the cavity can be estimated based on the volume admitted, see figure 1. In Figure 1, $\Delta avg \neq \Delta 1 \neq \Delta 2 \neq ... \Delta n$.

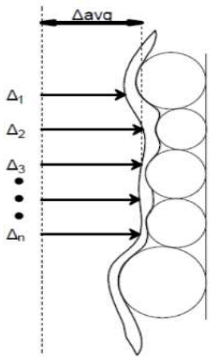

Figure 1. Resolution loss when calculating radial displacement by measuring volume injection.

When using strain gauges, the precision in estimating the horizontal strains improves considerably. This phenomenon should not be new to geotechnical engineers as a similar problem occurs when trying to estimate small strain stiffness in a triaxial probe as discussed by Jardine (1984). The improvement in resolution implies that the cavity expansion or contraction problem can be approached in a radically different form as previously treated by Ménard and his empirical expressions. In this case an analogy can be drawn with the SPT, which no geotechnical engineer would consider interpreting for deriving load-deformation curves. Although such an attempt might seem "feasible" – since both the load and the resulting displacement are known – it would inevitably fail due to resolution limitations.

In addition to the resolution issues, the pressuremeter curve presents a second significant challenge for interpretation: the complexity of soil behavior when attempting to reduce the boundary value curve measured by the instrument to the single-element response required for design. Many authors have developed analytical formulations for solving this problem and hence deriving geotechnical properties from the pressuremeter curves (Hughes et al., 1997, Palmer, 1972 and Bolton & Whittle, 1999) but the extent to which analytical expressions can be applied is limited and important simplifications to soil behaviour have to be made in order to resolve the mathematics involved. Others have resorted to numerical formulations (Manassero, 1989; Yu, 1990) improving the accuracy of the soil model but nowadays, only finite element or finite difference models can capture the full complexity of soil behaviour.

The rise of high resolution pressuremeters in recent years and the advent of modern and fast computers and finite element models (FEM) has allowed geotechnical engineers to model the test and back-analyse it in order to estimate the soil properties (Rui & Yin, 2018; Oztoprak & Bolton, 2010; Oztoprak et al. 2018). The authors have been using this procedure for some years with some success (Mella, 2022; Jara, 2023) but the progress has been restraint by (1) the long duration of the multiple software iterations needed to obtain a proper curve match and (2) non-uniqueness, i.e., the fact that a single curve can be matched by more than one set of soil properties and only few or one of them relates to the actual soil behaviour. These two difficulties can be eased by the use of the Artificial Intelligence (AI) software DAARWIN as explained in detail in this paper.

In order to assess the applicability of performing a geotechnical characterisation by means of modelling a high resolution pressuremeter curve, 4 pressuremeter tests were analysed. The first one was obtained by a pushed-in, high resolution pressuremeter testing a dry pluviated, controlled clean sand with well document geotechnical properties placed into a calibration chamber. The 3 other curves were obtained from calibration chambers obtained from the literature: one corresponds to a self-boring pressuremeter and the remaining two to cone pressuremeters. It will be shown that the proposed method is able to accurately reproduce the geotechnical properties and also the state parameter and in-situ lateral earth pressure, even in the cases when the tests were pushed-in.

2. DAARWIN

DAARWIN is a cloud-based platform based on machine learning genetic algorithms that gathers data, creates connections between design and construction, visualizes construction performance against design analysis, enables 'real-time' back-analysis to enable modifications to design and construction to be made based on actual performance, and better manage risk during underground construction (De Santos 2015).

DAARWIN refines geotechnical design models using data collected from site. It compares the design prediction against the measured response to enable a more accurate understanding and future analysis of the ground and ground-structure interaction behaviours. The resulting back-analysed parameters can be used for further designs, as well as for modifying the existing design and construction sequence through the application of the Observational Method (Peck, 1969) to make them more sustainable, efficient and safer.

Back-analysis is the process where model parameters are changed until an improved match with monitoring data is achieved. Once validated, the model can be extrapolated to predict ground and structural behaviour under varying conditions. Back-analysis is traditionally performed manually following trial-and-error. With the number of parameters in ground models increasing (especially for more advanced constitutive models), back-analysis typically takes three to six weeks. Accelerating back-analysis to near real-time using DAARWIN has the potential to transform geotechnical practice, and significantly enhances the power of the Observational Method. Because DAARWIN is also a data management platform it can also be a valuable repository of geotechnical information which, if used wisely, can be used to create leaner future designs.

Although DAARWIN was mainly developed for back-analysing monitoring data of geotechnical structures this work explores its application for interpreting pressuremeter data.

3. Calibration chamber and material used

Schnaid (1990) reported minor boundary effects observed in loose samples when the ratio of calibration chamber diameter to pressuremeter diameter exceeds 20. Based on these results, a calibration chamber 1.2m internal diameter, 12mm thick, A36 steel calibration chamber was built specifically for this study. As the chamber has not been instrumented yet, in order to measure the at-rest lateral earth pressure a first stage measuring process was devised. In this stage the Cambridge In-situ, 47mm diameter, Reaming Pressuremeter equipped with 3 strain gauges with a 1-micron resolution was placed prior to the soil sample, as illustrated in Figure 2. After the instrument is installed, the soil is placed by dry pluviation into the chamber around the pressuremeter in 0.3m thick layers. Each layer is poured from a constant height of 1.5m by means of a container that hangs from a bridge crane. The sand pours through a hose which can be closed with a valve (see Figure 3). After the chamber has been filled, a soil height of 1.05m rests above the pressuremeter pressure sensor. At this point a full test is carried out with special focus on the first part so that the lift-off pressure that represents the at-rest lateral pressure can be determined.

Figure 2. Calibration chamber with the pressuremeter installation prior to soil sample preparation– perfect installation.

Figure 3. Container hanging from bridge crane, hose with valve.

After the first pressuremeter test stage (perfect installation), the pressuremeter is withdrawn and a 50.8mm outer diameter, 1.5mm thick, hollow steel tube is pushed into the same soil sample. The steel tube is fitted with a 50.8 diameter cone tip that disconnects from the tube when it is lifted, allowing the pressuremeter to be inserted into the hollow tube so that the tube can then be withdrawn, leaving the pressuremeter in place for performing a second test. In this manner, the first test serves mainly for measuring the at-rest lateral earth pressure while it is the second test —conducted after tube withdrawal— is used for performing the analyses considered to reproduce a commercial test characterised by considerable soil disturbance during installation.

Following the second test, natural unit weight measurements were carried out at 4 different heights within the calibration chamber by extracting sand from top to bottom so as to access the various layers. The unit weights were measured by means of the sand cone method (ASTM D698-12e2. 2012). A representative dry unit weight of 14.4 kN/m^3 and a moisture content of 5% were obtained.

3.1. Soil properties

The tested material is an alluvial quaternary sediment from a volcanic origin, locally known as Biobío sand, owned to the river where the sediments are transported. Its mineralogy is mainly composed of basalt and feldspar. The grain size distribution of Biobío sand is distributed between silty sand and clean, poorly graded sand. The index properties are emin = 0.718, emax = 0.956, specific gravity (GS) of 2.79, coefficient of curvature (Cu) and uniformity (CC) of 0.97 and 2.29, respectively. A preliminary qualitative analysis of the sand particles classifies this material as a sub-angular shape (Kuncar et al., 2024).

According to a comprehensive laboratory testing program based on triaxial and oedometer tests carried out by Kuncar et al. (2024), the soil parameters presented in Table 1 based on the Clay and Sand Model (CASM) (Yu, 1995, 1998) can be determined:

Table 1. Biobio Sand properties

Parameters	Symbol	BB Sand
Slope of the compression line	λ	0.0248
Poisson's ratio	ν'	0.3
Shear strength angle at CS	ϕ'	32
Plastic Potential	m	2.9
Specific volume	Γ	1.99
Spacing ratio	r	*
Slope of the swelling line	κ	*
Parameter defining the shape	n	*

* Parameters not defined by Kuncar et al. 2024.

The lift-off pressure measured by the first-stage pressuremeter test is presented in Figure 4 and corresponds to an at-rest lateral earth pressure of σ_{h0} = 10.72kPa.

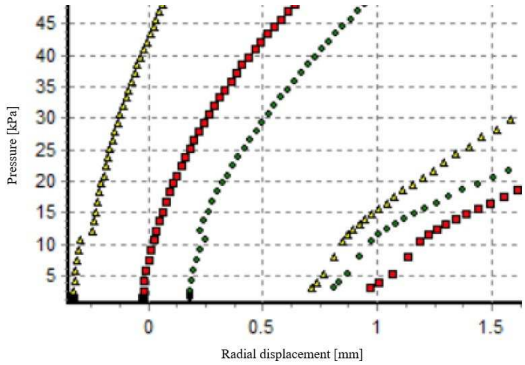

Figure 4. Lift-off pressure from perfect installation pressuremeter test at 10.72kPa.

With the above mentioned parameters and the dry unit weight measured at the chamber after both pressuremeter tests were carried out, the state parameter (ψ_0) can be determined as:

$e_{chamber} = G_s*\gamma_w/\gamma_d - 1 = 0.94$

$p' = (1.05*14.4*1.05+2*10.72)/3 = 12.19kPa$

$e_{CS} = 0.99-0.0248*\ln(p') = 0.93$

$\psi_0 = 0.94-0.93 = 0.010$

4. Literature tests

Three additional pressuremeter tests reported in the literature have been selected for this study. Their properties are presented in Table 2 (Li et al. 2024):

Table 2. Literature tests

Reference	Soil parameters	Test/type
Ticino sand (Bellotti et al. 1987)	*Γ = 1.986, λ = 0.024, κ = 0.008, ϕ= 34°, ν = 0.3, n= 2.0, r= 108.6*	*T246/SBP*
Leighton Buzzard sand (Schnaid 1990)	*Γ =1.8, λ = 0.025, κ = 0.005, ϕ= 33°, ν= 0.37, n= 2.0, r= 33*	*15CPMT03 /CPMT 15CPMT04/CPMT*

Note: SBP= Self-boring; CPMT= Cone pressuremeter

5. Pressuremeter Interpretation method

The method consists in modelling with an axisymmetric mesh in Plaxis 2D each pressuremeter test to be interpreted. For this study's calibration chamber, for example, a 30m wide by 4m deep mesh was used. This mesh size resulted in a better numerical convergence than actually modelling the chamber dimensions. Simulating the cavity pressure, a uniformly distributed pressure was applied at the test depth at a length of 0.255m which corresponds to the membrane length, see figure 5, i.e, the model is stress-controlled. Once the model is run with initial soil parameters chosen by the user, it needs to be uploaded to the Artificial Intelligence optimization algorithm (DAARWIN).

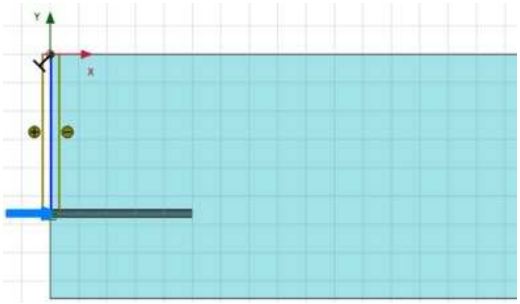

Figure 5. Pressuremeter test model

When using DAARWIN, the pressuremeter curve is treated as in the Observational Method. Assuming the pressuremeter as an inverse boundary value problem, the pressure-deformation data measured in-situ correspond to the target values and the soil parameters are the variables to be iterated to obtain the best fit as in a back-analysis. A critical input when deciding which data points to interpret is stablishing the deformation level at which the insertion disturbance has been "erased". This decision is based on the stabilisation of the slope from the unload-reload loops. Beyond the deformation level at which unload–reload loops provide consistent estimates of the elastic modulus during the pressuremeter expansion phase, the measured data points are used as input for the back-analysis. Conversely, all data points from the contraction phase are incorporated in their entirety. It can be argued that the slope of the unload-

reload loops depends on pressuremeter insertion disturbance level, strain amplitude and cavity pressure. If strain amplitude is held constant for all loops, then only disturbance and cavity pressure affect the loop slope. In this manner, if a relationship for the shear modulus and cavity pressure is derived based on the data for the last loop, a disturbance rate given by the percentual difference between the slope of the current loop and the derived from the last loop can be calculated. This disturbance rate can be assed for deciding a limit at which the pressuremeter data can be relied on to feed the AI-aided FEM method. The model for correcting by cavity pressure is shown in Eq. (1) and is taken from Belloti et al (1989):

$$G_{ln} = G_{measured} * \left(\frac{\sigma_{l3}}{\sigma_{ln}}\right)^{0.5} \quad (1)$$

Where:

G_{ln}: shear modulus from loop n.
$G_{measured}$: shear modulus measured at loop 3.
σ_{l3}: cavity pressure at loop 3.
σ_{ln}: cavity pressure at loop n.

This procedure has been applied to a perfect installation test and to a pushed-in test shown in Figure 6. Table 3 presents the disturbance rate assuming the third loop for each test has zero disturbance rate.

Table 3. Disturbance rate per loop

Test	Loop	Cavity pressure (kPa)	Disturbance rate (%)
Perfect Installation	1	112	16.2
	2	135	8.0
	3	160	0
Pushed-in	1	84.3	30.0
	2	136.5	10.9
	3	171.8	0

From Table 3 it is evident that the perfect installation method exhibits less disturbance than the pushed-in method for loop 1, although some experimental disturbance is still present (16.2%). For loop 2, however, most of the disturbance has been "erased" for both tests (<11%), which is a good indicator that after some additional pressure most of the disturbance will be overcome.

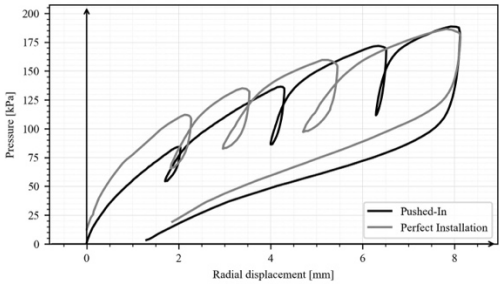

Figure 6. Perfect Installation and pushed-in tests.

In contrast to other soil constitutive models, it has been observed by the authors that by using DAARWIN with CASM a better fit is obtained by letting the software freely iterate all CASM's parameters. On the other hand, in the case of using the Hardening Soil Small Strain (HSS) model, for example, a better fit is obtained if the shear modulus at small strains (G0) is input as a known variable (see companion paper for this conference, Martinez et al, 2025).

The principle behind the idea of determining Ko and ψ_0 for a pre-bored or pushed-in instrument is that although the soil element immediately at the cavity wall has been disturbed, there are elements away from the wall that have not been disturbed by the insertion process. As the pressuremeter test stresses several soil elements close and away from the cavity wall, the measured curve is also shaped by those elements away from the wall and their parameters can be recovered.

An apparently similar, but in reality very different, study was undergone by Li et al. (2024). They used a semi-analytical method that combines cavity expansion and contraction for predicting K_0 and ψ_0. Their method needs as an input the values of ϕ, λ, κ, Γ, n, r and ν and so by adjusting the values of K_0 and ψ_0 a best fit to the measured curve is sought. The present method, in contrast, does not need the aforementioned parameters as input, they are also a result of the interpretation method and their determination responds to an optimization algorithm that minimizes the sum of the squares due to regression (SSR).

5.1. Results

5.1.1. This study's Calibration chamber

The perfect installation and pushed-in pressuremeter curves measured are presented in figure 7.

The CASM soil parameters interpreted by the herein described method are presented in table 3.

Table 4. Back-analysed test results

Parameters	Symbol	BB Sand	Pushed-in interpretation
Slope of the compression line	λ	0.0248	0.022
Poisson's ratio	ν'	0.3	0.3
Shear strength angle at CS	ϕ' (°)	32	32
Plastic Potential	m	2.9	3.7

Specific volume	Γ	1.99	2.12
Spacing ratio	r	*	49
Slope of the swelling line	κ	*	0.0036
Parameter defining the shape	n	*	3
State parameter	ψ_0	0.010	0.012
At-rest lateral earth pressure	σ_{h0} (kPa)	10.72	10.80
At-rest lateral earth pressure coefficient	K_0	0.68	0.68
Sum of squares regression	SSR		1.226

* Not defined by Kuncar et al. 2024.

The measured and back-analysed data are presented in Figure 7. In this and subsequent figures the black dots represent the input data provided to the AI model, whereas the grey squares are the results of the interpretation. It can be observed in this figure that for the expansion phase - based on the disturbance rate criterion discussed earlier - only data beyond approximately 6.0mm of radial displacements were used as input for analysis. The insert in Figure 7, as well as those in subsequent figures, provide a zoomed view of the results at small deformations. Notably, the lift-off pressure recorded by the pressuremeter does not correspond to the lateral pressure of 10.72kPa established under perfect installation conditions. However, the interpreted curve yields a pressure of 10.80kPa at zero radial displacements, which closely matches the measured value.

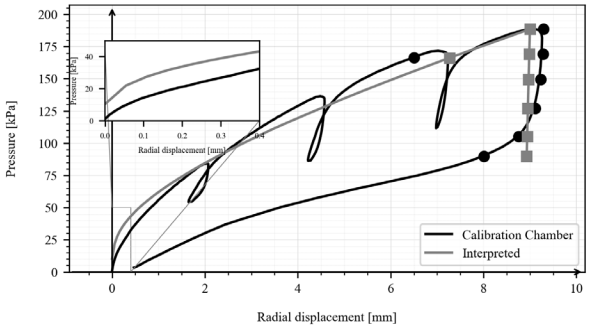

Figure 7. Measured and back-analysed curves – calibration chamber

5.1.2. Test T246 (SBP)

The CASM soil parameters interpreted are presented in Table 4 and the measured and back-analysed data are compared in Figure 8. It is interesting to note that despite the use of a self-boring pressuremeter, significant disturbance is still evident at the beginning of the test, as illustrated in the insert of Figure 8. The lift-off pressure from the SBP does not correspond to the lateral pressure of 52.97kPa determined by the chamber readout, whereas the interpreted curve yields a pressure of 51.65kPa, which is remarkably close to the measured value.

Table 5. Back-analysed test results

Parameters	Symbol	T246	Interpretation
Slope of the compression line	λ	0.024	0.034
Poisson's ratio	ν'	0.3	0.3
Shear strength angle at CS	ϕ' (°)	34	34
Plastic Potential	m	*	2.8
Specific volume	Γ	1.99	1.82
Spacing ratio	r	109	101
Slope of the swelling line	κ	0.0080	0.0087
Parameter defining the shape	n	2.0	1.3
State parameter	ψ_0	-0.13	-0.004
At-rest lateral earth pressure	σ_{h0} (kPa)	52.97	51.65
At-rest lateral earth pressure coefficient	K_0	0.52	0.51
Sum of squares regression	SSR		0.061

*Not defined by Li et al. 2024

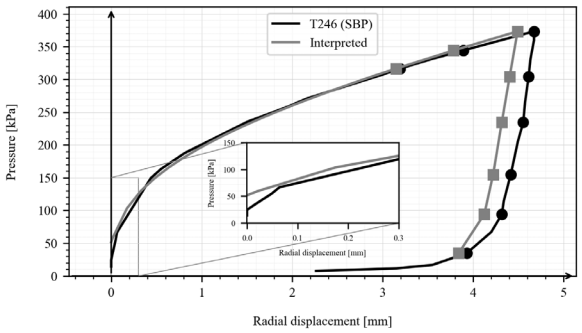

Figure 8. Measured and back-analysed curves – T246 (SBP).

5.1.3. Test 15CPMT04 (Loose state)

The CASM soil parameters interpreted are presented in Table 5 and the measured and back-analysed data are presented in Figure 9. As this test is a cone pressuremeter characterised by considerable insertion disturbance, only the contraction data is back-analysed.

Table 6. Back-analysed test results

Parameters	Symbol	15CMPT04	Interpretation
Slope of the compression line	λ	0.025	0.046
Poisson's ratio	ν'	0.37	0.30

Shear strength angle at CS	ϕ' (°)	33	31
Plastic Potential	m	*	2.2
Specific volume	Γ	1.80	1.61
Spacing ratio	r	33	30
Slope of the swelling line	κ	0.0050	0.0065
Parameter defining the shape	n	2.0	1.9
State parameter	ψ_0	0.020	0.12
At-rest lateral earth pressure	σ_{h0} (kPa)	96.60	100.80
At-rest lateral earth pressure coefficient	K_0	1.08	1.13
Sum of squares regression	SSR		1.077

*Not defined by Li et al. 2024

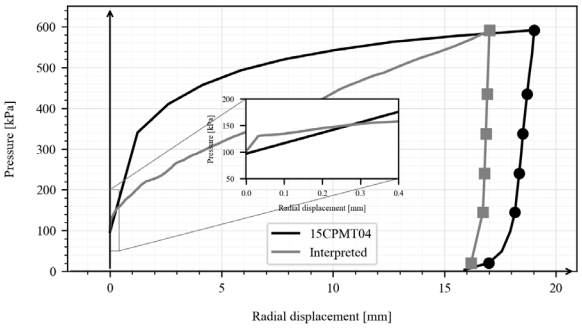

Figure 9. Measured and back-analysed curves – 15CMPT04 (loose)

5.1.4. Test 15CPMT03 (Dense state)

The interpreted CASM soil parameters are presented in table 6 and the measured and back-analysed data are presented in figure 10. As this test is a cone pressuremeter characterised by insertion disturbance, only the contraction data in back-analysed.

Table 7. Back-analysed test results

Parameters	Symbol	15CMPT03	Interpretation
Slope of the compression line	λ	0.025	0.049
Poisson's ratio	ν'	0.37	0.30
Shear strength angle at CS	ϕ' (°)	33	31
Plastic Potential	m	*	5.6
Specific volume	Γ	1.80	1.71
Spacing ratio	r	33	30
Slope of the swelling line	κ	0.0050	0.0054
Parameter defining the shape	n	2.0	1.0
State parameter	ψ_0	-0.11	-0.003
At-rest lateral earth pressure	σ_{h0} (kPa)	96.60	74.37
At-rest lateral earth pressure coefficient	K_0	1.08	0.83
Sum of squares regression	SSR		0.262

*Not defined by Li et al. 2024

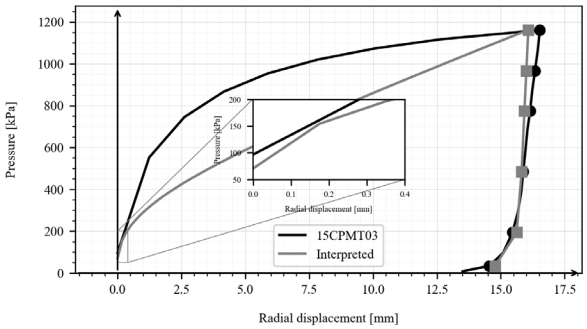

Figure 10. Measured and back-analysed curves – 15CMPT03 (dense).

Figure 11 and 12 present the summary of results for the at-rest lateral earth pressure and state parameter respectively.

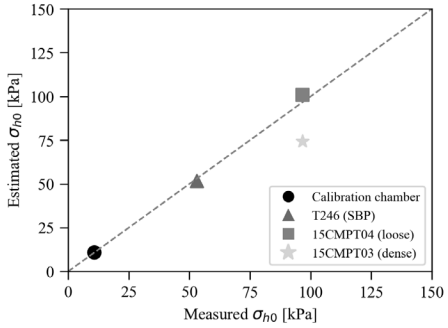

Figure 11. Summary of results: at-rest lateral stress.

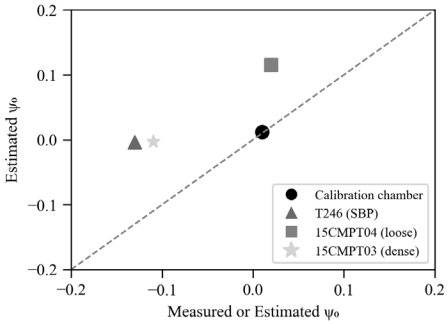

Figure 12. Summary of results: state parameter.

6. Conclusions

This paper presents a method for interpreting pressuremeter tests affected by installation disturbance using Artificial Intelligence to estimate soil properties and in situ stresses. The approach is based on numerical modelling of four pressuremeter obtained from tests conducted in calibration chambers with well characterised materials. Each pressuremeter test was modelled using an axisymmetric mesh in Plaxis 2D with soil properties for each case determined through back-analysis of the pressuremeter curve using an AI-aided software called DAARWIN. The results demonstrate that the proposed method accurately estimates soil parameters, which were independently assessed from laboratory tests. Additionally, the state parameter is reasonably well estimated while the at-rest lateral earth pressure is calculated with remarkable precision. These good results are obtained independently if the tests are self-bored or pushed-in, which confirms the assumption that the method can deal with initial cavity disturbance.

A notable advantage of using pressuremeters in conjunction with finite element models is that constitutive models are calibrated as a whole with all soil parameters being properly interconnected to reproduce the full stress-strain response - an outcome not achievable through conventional SPT or CPTu tests. The mathematical simplifications historically used to reduce the boundary value problem to a single-element curve can be bypassed, allowing for more sophisticated and realistic soil models. This leads to more accurate prediction of geotechnical properties. Consequently, the proposed method is well suited for geotechnical design applications, including dams, slopes, piles, and foundations, and is applicable to a wide range of geomaterials such as residual soils, heavily weathered rock, gravels, and clays, given that the pressuremeter is an in situ test capable of being installed in different ground conditions.

Acknowledgements

The authors would like to thank Cristian de Santos CEO at SAALG Geomechanics, Berta Solá and Laia Gelonch Geotechnical Engineers at SAALG Geomechanics for their support and advice using DAARWIN.

References

Ajalloeian, R., & Yu, H. (1998). Chamber studies of the effects of pressuremeter geometry on test results in sand. Géotechnique/Geotechnique, 48(5), 621-636. https://doi.org/10.1680/geot.1998.48.5.621

ASTM D698-12e2. (2012). Standard Test Methods for Laboratory Compaction Characteristics of Soil Using Standard Effort (12,400 ft-lbf/ft³ or 600 kN-m/m³). ASTM International, West Conshohocken, PA. https://doi.org/10.1520/D0698-12E02

Belloti, R., Ghionna, V., Jamiolkowski, M., Robertson, P., Peterson., R., (1989) Interpretation of moduli from self-boring pressuremeter tests in sand Géotechnique Vol.XXXIX, no.2, pp. 269-292.

Bolton, M. D., & Whittle, R. W. (1999). A non-linear elastic/perfectly plastic analysis for plane strain undrained expansion tests. Géotechnique/Geotechnique, 49(1), 133-141. https://doi.org/10.1680/geot.1999.49.1.133

De Santos C. Backanalysis Methodology Based on Multiple Optimization Techniques for Geotechnical Problems. Ph.D. thesis. Universitat Politècnica de Catalunya – BarcelonaTECH. 2015.

Houlsby, G. T., & Carter, J. (1993). The effects of pressuremeter geometry on the results of tests in clay. Géotechnique/Geotechnique, 43(4), 567-576. https://doi.org/10.1680/geot.1993.43.4.567

Hughes, J. M. O., Wroth, C. P., & Windle, D. (1977). Pressuremeter tests in sands. Géotechnique/Geotechnique, 27(4), 455-477. https://doi.org/10.1680/geot.1977.27.4.455

Jara, M. (2023). Modelamiento Numérico de un Muro Berlinés Caracterizado Mediante Datos de Presiómetro en Descarga. [Tesis de pre – grado para optar a título de Ingeniero Civil. Universidad de Concepción].

Jardine, R. J., Symes, M. J., & Burland, J. B. (1984). The Measurement of soil stiffness in the triaxial apparatus. Géotechnique/Geotechnique, 34(3), 323-340. https://doi.org/10.1680/geot.1984.34.3.323

Kuncar C., Escribano D., Montalva G. Obtaining critical state parameters through particle shape characteristics of sands. In: Proceedings of the 17th Pan-American Conference on Soil Mechanics and Geotechnical Engineering (XVII PCSMGE), La Serena, Chile, 2024.

Li G., Mo P., Lu Z., Yuan R., Yang H., Yu H. (2024). "Drained Cavity Expansion–Contraction in CASM and Its Application for Pressuremeter Tests in Sands", J. Geotech. Geoenviron. Eng., 150(9): 04024073, 2024. https://doi.org/10.1061/JGGEFK.GTENG-12417

Mair, R. J., & Wood, D. M. (1987). Pressuremeter testing: Methods and Interpretation. Butterworth-Heinemann.

Manassero, M. (1989). Stress-strain relationships from drained self-boring pressuremeter tests in sands. Géotechnique/Geotechnique, 39(2), 293-307. https://doi.org/10.1680/geot.1989.39.2.293

Martínez R., Jara M., Mántaras F., Odebrecht E. The use of Artificial Intelligence, Finite Element Modelling and Pressuremeter tests for geotechnical characterisation. In: Proceedings of the 8th International Symposiun on Pressuremeters, Luxembourg, 2025.

Mella, M. (2022). Análisis crítico de parámetros de deformación para la estimación de asentamientos en edificios en Concepción. [Tesis de pre – grado para optar a título de Ingeniero Civil. Universidad de Concepción].

Oztoprak, S. & Bolton, M. (2010). Parameter calibration of modified hyperbolic model for sands using pressuremeter test data. International Symposium on Deformation Characteristics of Geomaterials, September 1-3, 2010, Seoul, Korea.

Oztoprak, S., Sargin, S., Uyar H., & Bozbey I. (2018). Modeling of pressuremeter test to characterize the sands. Geomechanics an Engineering, Vol. 14, No 6 (2018) 509-517. https://doi.org/10.12989/gae.2018.14.6.6.509

Palmer, A. (1972). Undrained plane-strain expansion of a cylindrical cavity in clay: a simple interpretation of the pressuremeter test. Géotechnique/Geotechnique, 22(3), 451-457. https://doi.org/10.1680/geot.1972.22.3.451

Peck, R. B. (1969). Advantages and limitations of the observational method in applied soil mechanics. Geotechnique, 19(2), 171-187. https://doi.org/10.1680/geot.1969.19.2.171

Rui, Y., & Yin, M. (2018). Interpretation of pressuremeter test by finite-element method. Proceedings Of The Institution Of Civil Engineers. Geotechnical Engineering/Proceedings Of ICE. Geotechnical Engineering, 171(2), 121-132. https://doi.org/10.1680/jgeen.17.00032

Schnaid F. "A study of the cone-pressuremeter test in sand", Phd thesis, University of Oxford, 1990.

Yu, H.S. (1990). "Cavity Expansion Theory and its Application to the Analysis of Pressuremeters", DPhil Thesis, University of Oxford.

Yu, H. S., 1995, A unified state parameter model for clay and sand. Civil Engineering Research Report No. 112.08.1995. NSW, Australia: University of Newcastle.

Yu, H. S., 1998, CASM: A unified state parameter model for clay and sand. International Journal for Numerical and Analytical Methods in Geomechanics, 22(8), 621-653.